Title
Shear stress induced by fluid flow produces improvements in tissue-engineered cartilage.

Journal
Biofabrication, 12(4)

ISSN
1758-5082

Authors
Salinas, EY
Aryaei, A
Paschos, N
et al.

Publication Date
2020-08-01

DOI
10.1088/1758-5090/aba412

Peer reviewed

PAPER

Shear stress induced by fluid flow produces improvements in tissue-engineered cartilage

IOP Publishing Biofabrication 12 (2020) 045010 https://doi.org/10.1088/1758-5090/aba412

Biofabrication

PAPER

Shear stress induced by fluid flow produces improvements in tissue-engineered cartilage

E Y Salinas[1,5], A Aryaei[2,5], N Paschos[3], E Berson[4], H Kwon[1], J C Hu[1] and K A Athanasiou[1]

[1] Department of Biomedical Engineering, University of California Irvine, 3131 Engineering Hall, Irvine, CA, 92697, United States of America
[2] Boston Scientific Corporation, San Jose, California, United States of America
[3] Department of Orthopedic Surgery, Division of Sports Medicine, Harvard Medical School, Boston, MA, United States of America
[4] Department of Chemical Engineering, University of Louisville, Kentucky, United States of America
[5] Authors contributed equally to this work

E-mail: e.y.salinas@uci.edu, ashkan.aryaei@gmail.com, paschos.nikolaos@gmail.com, eric.berson@louisville.edu, heenam.kwon@uci.edu, jerryhu@uci.edu and athens@uci.edu

RECEIVED
3 March 2020

REVISED
15 June 2020

ACCEPTED FOR PUBLICATION
8 July 2020

PUBLISHED
28 July 2020

Keywords: tissue engineering, biomaterial, mechanical stimulation, fluid flow, neocartilage

Supplementary material for this article is available online

Abstract

Tissue engineering aims to create implantable biomaterials for the repair and regeneration of damaged tissues. *In vitro* tissue engineering is generally based on static culture, which limits access to nutrients and lacks mechanical signaling. Using shear stress is controversial because in some cases it can lead to cell death while in others it promotes tissue regeneration. To understand how shear stress works and how it may be used to improve neotissue function, a series of studies were performed. First, a tunable device was designed to determine optimal levels of shear stress for neotissue formation. Then, computational fluid dynamics modeling showed the device applies fluid-induced shear (FIS) stress spanning three orders of magnitude on tissue-engineered cartilage (neocartilage). A beneficial window of FIS stress was subsequently identified, resulting in up to 3.6-fold improvements in mechanical properties of neocartilage *in vitro*. *In vivo*, neocartilage matured as evidenced by the doubling of collagen content toward native values. Translation of FIS stress to human derived neocartilage was then demonstrated, yielding analogous improvements in mechanical properties, such as 168% increase in tensile modulus. To gain an understanding of the beneficial roles of FIS stress, a mechanistic study was performed revealing a mechanically gated complex on the primary cilia of chondrocytes that is activated by FIS stress. This series of studies places FIS stress into the arena as a meaningful mechanical stimulation strategy for creating robust and translatable neotissues, and demonstrates the ease of incorporating FIS stress in tissue culture.

1. Introduction

All tissues in the body require nutrient and waste transport, as well as signal transmission via both soluble and mechanical cues. For example, vasculature, the most abundant source of transport and transmission in the body, delivers both soluble factors and mechanical signals via fluid-induced shear stress (FIS). *In vitro* tissue engineering has not typically incorporated vasculature and, instead, relies on static culture, limiting the transfer of soluble factors and removing fluid-induced mechanical signals. Static cultures are widely used in part because high-levels of shear have been associated with elevated levels of apoptosis [1], tissue degradation [2], and secretion of proinflammatory factors [3]. Specifically in chondrocytes, shear stress has been linked to upregulation of proinflammatory factors and pro-apoptosis, and in cartilage tissue, shear stress has been linked to matrix degradation [4, 5]. However, for some cells, such as vascular endothelial cells and cardiomyocytes [6], specific shear stress magnitudes have been identified as beneficial [2]. Motivated by the potential ease of using shear stress in tissue culture, we embarked on a comprehensive series of studies aimed to determine an optimal beneficial shear stress regimen, to

investigate the translatability of this strategy, and to explore how shear stress mechanistically improves tissue engineering.

To study how fluid flow may be used to enhance neotissue properties, we selected self-assembled neocartilage as a model [7, 8]. Neocartilage is the ideal model system for this series of studies because native articular cartilage does not rely on vasculature for survival. At the same time, cartilage, which is subjected to shear forces due to interstitial fluid flow, requires mechanical stimuli to maintain homeostasis [9]. Cartilage injuries constitute some of the most vexing medical problems because of the tissue's innate inability to heal [10], making it a prime candidate for tissue engineering [11]. To restore cartilage's biomechanical function, the use of tissue-engineered neocartilage as a model system holds clinical promise and translational potential for the 240 million people that suffer from articular cartilage degeneration worldwide [2]. Establishing FIS stress as a potent mechanical stimulation strategy in tissue engineering can contribute to the significant medical need for producing replacement cartilage.

Although native articular cartilage experiences shear stress, prior mechanical stimulation strategies have focused on applying hydrostatic pressure, compression, and recently, uniaxial tension, during tissue culture [12]. Optimal loading windows and, in some cases, cell-signaling pathways have been identified for these stimuli [13–15] but not for shear stress. Despite tantalizing hints of the ability of shear stress to improve tissue quality, such as collagen type II deposition [16–18], a window of shear stress for optimal tissue formation has yet to be identified. How FIS stress is transduced also remains largely unexplored for chondrocytes. Motivated by how shear stress loading maintains native articular cartilage, we sought to identify a window of FIS stress magnitude that produces neocartilage robust enough to thrive in an *in vivo* environment. We also sought to elucidate the players in mechanotransducing shear stress toward enhanced neocartilage construct properties. Toward translation and demonstration that the stimulus functions across species, we also aimed to employ FIS stress to produce human neocartilage.

In this series of studies, we designed and developed a device that applies shear stress to neocartilage by using an orbital shaker to create oscillatory fluid motion. The neocartilage is held in fixed positions as fluid flows over it, creating shear stress on the surface of the neocartilage constructs. We also identified an optimized FIS stress loading regimen on neocartilage and investigated a cell signaling pathway involved in producing improved extracellular matrix properties (figure 1). We used computational fluid dynamics (CFD) models to quantify the magnitudes of FIS stresses that were applied on neocartilage constructs with parameters including settings on the orbital shaker and location in the device. Contrary to the prevailing notion of avoiding shear stress in cartilage tissue culture [1, 19, 20], we hypothesized that a window of shear stress could be identified that leads to the enhancement of collagen content and mechanical properties of neocartilage. We then performed an *in vivo* rat study to examine whether FIS stress-induced improvements in neocartilage mechanical properties could be maintained for 8 weeks; another objective of the *in vivo* study was to test the hypothesis that implanted neocartilage extracellular matrix and cellular organization would remodel toward mature native tissue properties. Subsequently, we translated the optimal FIS stress loading conditions to engineer human neocartilage. We also examined how FIS stress initiates mechanotransduction to improve neocartilage properties. To elucidate how FIS stress contributed to the observed results, we performed RNA sequencing and scanning electron microscopy imaging. The overall objective of this work was to establish FIS stress as a meaningful mechanical stimulation strategy for creating robust and translatable neocartilage, as well as to demonstrate the ease and benefit of incorporating FIS stress in tissue culture.

2. Materials & methods

2.1. Bovine chondrocyte harvest

Juvenile bovine (14–30 d) stifle joints were procured from Research 87. Articular cartilage was harvested from the distal femurs within 48 h of slaughter. The harvested articular cartilage was digested in 0.2% collagenase type II (Worthington Biochemical Corp) solution for 18 h to release the chondrocytes from the tissue matrix. Next, the chondrocytes were washed in a solution of Dulbecco's Modified Eagle's Medium (DMEM) and 1% penicillin-streptomycin-fungizone (PSF, Lonza BioWhittaker). For each study in this investigation, eight juvenile bovine stifle joints were used; chondrocytes from the eight animals were pooled and counted using a hemocytometer, and their viability was estimated using a trypan blue exclusion assay. Cells were stored at −80 °C in freezing medium containing 90% fetal bovine serum and 10% dimethyl-sulfoxide serum until use.

2.2. Human chondrocyte harvest and expansion

Human knee articular chondrocytes were harvested from a Caucasian male donor, age 43, with no known musculoskeletal pathology (Musculoskeletal Transplant Foundation). The human chondrocytes were passaged and chondrotuned as previously described [15]. Briefly, the chondrocytes were expanded in a chondrogenic culture medium with bioactive factors TGF-β1 (1 ng ml^{-1}), bFGF (10 ng ml^{-1}), and PDGF-bb (10 ng ml^{-1}) (all from Peprotech) to passage 3. Cells were then placed in a 3D aggregate culture for a duration of 7 d [15]. The resulting aggregates were digested using 0.2% collagenase to release the redifferentiated chondrocytes for construct seeding [8].

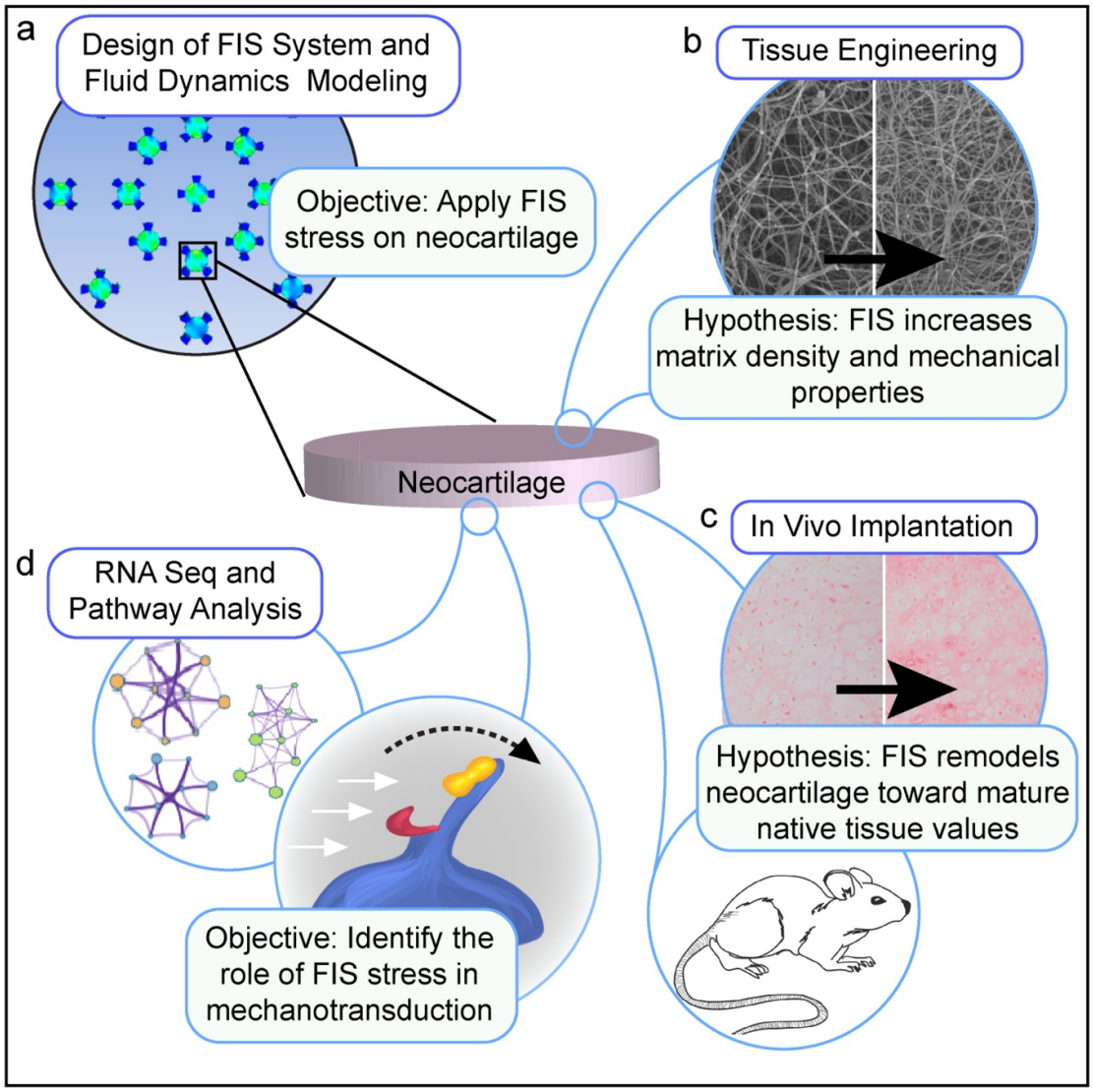

Figure 1. Overview of series of studies to elucidate the roles of fluid-induced shear (FIS) stress. (a) Computational fluid dynamics models to determine shear stress magnitude imparted on neocartilage in the FIS stress device. (b) Tissue engineering studies *in vitro* using bovine and human cells to test the hypothesis that FIS stress results in enhancements in neocartilage density and mechanical characteristics. (c) *In vivo* studies in athymic mice to test the hypothesis that FIS stress-stimulated neocartilage remodels toward native values after implantation. (d) RNA sequencing followed by pathway analysis to elucidate mechanotransduction pathways activated by FIS stress.

2.3. The self-assembling process

Before seeding, 5 mm diameter, non-adherent, sterilized, agarose (2% weight/volume phosphate-buffered saline (PBS)) wells were formed and pre-saturated with chondrogenic medium (DMEM with GlutaMAX (Gibco); nonessential amino acids (0.1 mM) (Gibco); 1% insulin, human transferrin, and selenous acid (ITS+; BD Biosciences); 1% PSF; dexamethasone (100 nM) (Sigma-Aldrich); ascorbate-2-phosphate (50 μg ml^{-1}) (Sigma-Aldrich); sodium pyruvate (100 μg ml^{-1}) (Sigma-Aldrich) and L-proline (40 μg ml^{-1}) (Sigma-Aldrich). In the non-adherent, agarose wells 4 million chondrocytes were seeded to form self-assembled, scaffold-free, neocartilage constructs; the constructs were fed 0.5 ml of chondrogenic medium daily. Once the neocartilage constructs grew to the edge of the agarose wells (day 7), they were transferred to the FIS stress stimulation device. The neocartilage constructs have not been shown to grow significantly in diameter or thickness during culture under FIS. After FIS stress stimulation, constructs were transferred to a 48-well tissue culture treated plate and maintained in static culture with 1 ml of chondrogenic medium exchanged per day for the remaining culture duration (total culture time = 28 d). For experimental groups treated with bioactive factors, TGF-β1 and LOXL2 were used. TGF-β1 (10 ng ml^{-1}) was applied continuously. LOXL2 was applied on days 15–28 (0.15 μg ml^{-1}) (SignalChem) with copper sulfate (1.6 μg ml^{-1}) (Sigma-Aldrich) and hydroxylysine (0.146 μg ml^{-1}) (Sigma-Aldrich). For human-derived neotissues, C-ABC (Sigma-Aldrich)(2 U ml^{-1}) CHG was applied for 4 h on day 7.

2.4. FIS stress device fabrication

The FIS stress device was made by first fabricating an acrylonitrile butadiene styrene (ABS) negative mold using the additive manufacturing process of the open source MakerBot. The ABS negative mold was sterilized in an autoclave before every use. To create the FIS stress device, 23 ml of sterilized agarose in 2% weight/volume phosphate-buffered saline (PBS) was deposited into an 83 mm diameter petri dish. The ABS negative mold was then placed on top of the agarose. Once the agarose gelled (15 min), the ABS negative mold was removed and the resultant FIS stress device remained in the petri dish (figures 2(a)–(d)). Agarose was used to create the device because of its cost effectiveness, and in order avoid rusting that results from using steel in a humid culture environment. Additionally, agarose is non-adherent to cells and not a barrier to nutrient diffusion, as opposed to steel or acrylic. To induce FIS stress, the device was first saturated with chondrogenic medium through three exchanges of 20 ml of the medium, then filled with 20 ml of the medium and placed on an orbital shaker at 25, 50, or 100 RPM. Because the petri dish is only 100 mm in diameter and a standard orbital shakers, 500 × 500 mm, can hold a single layer of about 20 petri dishes. The petri dishes may also be stacked, meaning over 20 petri dishes can be mounted on the shaker at the same time.

2.5. Computation of shear stress in device

The unsteady, free-surface flow inside the device was modeled by solving three-dimensional Navier–Stokes equations using the commercial CFD software ANSYS FLUENT 16.1. Three-dimensional cylindrical renderings of the neocartilage constructs and the device were generated using the preprocessor ANSYS ICEM CFD 16.1. Certain CFD modeling parameters, including the dimensions of the neocartilage constructs, the dimensions of the device, and the orbital diameter, were held constant as follows: The diameter of the device was 83 mm with 16 cylindrical constructs, each supported and held in place by four posts. Each neocartilage construct, modeled as a solid cylinder with a radius of 2.5 mm and a thickness of 0.7 mm, was supported by four posts that were 1.5 mm thick and 4.8 mm tall, in the positions shown in figure 2(d). The orbital diameter was set to fit the standard orbital shaker size of 19 mm. Theoretically, changes in the parameters that were held constant for the *in vitro* portion of this study; such as construct and device size and geometry may alter the shear stress generated in the device. However, previous studies have shown that to create a significant difference in the generated shear stress, the device would have to double in diameter [21]. Finally, the independent variables examined were orbital velocity at orbital shaker settings of 25, 50, or 100 RPM and an inner or outer position on the device. An unstructured mesh of 1 001 750 tetrahedral shaped cells was applied to the volume. A higher mesh density was applied to the constructs, versus the bulk region, for proper resolution.

The volume of fluid (VOF) model was applied to track the liquid-air interface present in the system. In the model, both phases sharing the interface employed a combined set of momentum equations so that the volume fraction of each fluid in each cell can be tracked throughout the grid. The two phases were set with the default properties for air and water. The initial resting liquid height was set as 4 mm. The mesh's orbital motion was specified by a user-defined function. The three orbital RPMs yielded three separate cases of FIS stress magnitude; frequency was not measured because the frequency and magnitude cannot be controlled independently using this device. A time step of 0.0001 was determined to be necessary for acceptable convergence. Techniques for modeling and determining convergence criteria, grid optimization, and time needed to reach steady state for the transient solution have been previously described [22–24].

2.6. FIS stress stimulation

FIS stress stimulation was applied to neocartilage constructs starting at day 7. Five ranges of FIS stress magnitude were investigated by placing the device on the orbital shaker at 25, 50, or 100 RPM. The FIS stress device induced a range of 0–0.01 Pa at 25 RPM, ranges of 0.07–0.15 Pa and 0.05–0.21 Pa at 50 RPM, and ranges of 0.37–0.70 Pa and 0.25–0.85 Pa at 100 RPM (figures 3(a)–(c)). FIS stress stimulation durations of 6 d and 12 d were investigated.

2.7. Mechanical testing

A 2.5 mm diameter punch from the center of the neocartilage constructs was used for creep indentation testing using an automated indentation apparatus [25, 26]. Briefly, a 0.9 mm diameter, flat, porous, indenter tip was used to apply a 2 g (0.02 N) step mass onto the neocartilage construct to reach 10%–15% strain. The indented neocartilage was allowed to creep to equilibrium as described previously [27, 28]. The aggregate modulus and shear modulus were estimated by analyzing the experimental data using a semi-analytical, seminumerical, linear biphasic model in combination with finite element modeling [27].

Tensile testing samples were taken in the shape of a dog bone, following ASTM D3039 standards, with a gauge length of 1 mm. Paper was glued to the construct tabs outside the gauge and gripped by a mechanical tester (TestResources, Inc.). The construct was pulled apart at 1% of the gauge length per second (0.01 mm s^{-1}) until failure. Image-J was used to measure the cross-sectional area, and a stress-strain curve was generated to yield the tensile Young's modulus. The ultimate tensile strength (UTS) was obtained by measuring the maximum stress on the curve.

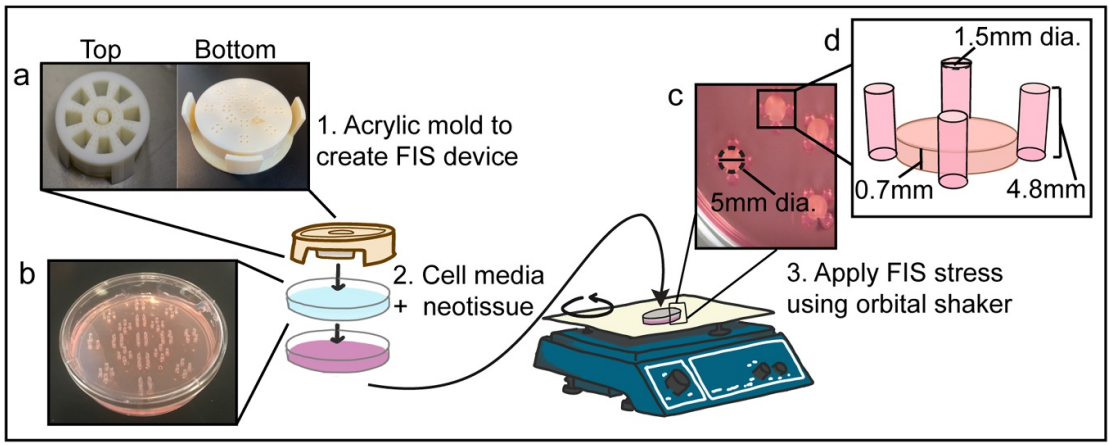

Figure 2. The fabrication and use of the FIS stress device (a) A 3D-printed acrylic mold was used to form the FIS stress device. (b) The FIS stress device was made of 2% agarose in a petri dish. A total of 16 constructs were held in place by four posts each. (c) The constructs were placed in the FIS stress device for 6 or 12 d after 7 d of initial culture, and the device was filled with cell media. Placing the device on an orbital shaker initiated FIS stress stimulation. (d) The neocartilage constructs sit in the device surrounded by four agarose posts that hold it in place.

2.8. Biochemical analysis

Samples were weighed, lyophilized for 72 h, weighed again, and digested in 125 μg ml^{-1} papain solution (Sigma), 2 mM N-acetyl cysteine (Sigma), and 2 mM EDTA (Sigma)) in phosphate buffer (50 mM, pH = 6.5) at 65 °C for 18 h. Total DNA was quantified using PicoGreen dsDNA reagent (Invitrogen). Total GAG content was measured using a Blyscan assay kit from Biocolor, and total collagen content was quantified using a modified colorimetric chloramine-T hydroxyproline assay [29]. For the collagen assay, a Sircol collagen standard (Biocolor) was used to create a standard curve.

2.9. Genomic analysis

mRNA was isolated immediately after FIS stress stimulation ceased using an RNeasy Kit (Qiagen, Inc.). mRNA from samples that were not stimulated with FIS stress was also isolated at the same time as samples stimulated with FIS stress. RNA-Seq was performed by the UCI Genomics High-Throughput Facility (GHTF). The RNA Sequencing libraries used by the UCI GHTF were prepared with the mRNA-Seq sample preparation kit from Illumina and sequenced using the Illumina HiSeq 2000. In total, eight constructs were sequenced (four stimulated with the optimal FIS stress loading, and four non-stimulated controls). After applying quality control filters, paired-end libraries were used to perform differential expression analysis on a Linux platform using the Hypergeometric Optimization of Motif EnRichment (HOMER) modules tools suite [30]. The NIH's Database for Annotation, Visualization and Integrated Discovery (DAVID) was used to translate gene identification numbers to genes names, and Cytoscape was used to perform pathway analysis and cluster genes of similar function.

RT-PCR was performed on the genes of interest: IHH, PKD1, and PKD2, which encode for PC1 and PC2, respectively. RT-PCR was performed on both human and bovine derived neocartilage. Total RNA was reverse-transcribed using random primers (Integrated DNA technologies), with GAPDH primers used to control for cDNA concentration in separate RT-PCRs for all samples. Primers for bovine GAPDH, IHH, PKD1, and PKD2, and human B2 M, IHH, PKD1, and PKD2 were designed using the Integrated DNA technologies PrimerQuest tool; they are shown in supplementary table 5 (available online at stacks.iop.org/BF/12/045010/mmedia). The specificity of all primers was verified to be 100% with the NIH's National Library of Medicine online Nucleotide Blast tool. PerfeCTa SYBR Green SuperMix from Quanta Bio was added to each RT-PCR reaction (plated in triplicate) for a total reaction volume of 25 ul. Ct values were normalized to GAPDH expression levels to obtain the relative expression of the gene of interest in comparison to GAPDH in both control and FIS-stimulated constructs.

2.10. *In vivo* study

The Institutional Animal Care and Use Committee (IACUC) of UC Davis approved the use of 12 6–8 week old athymic mice for this study. All neocartilage constructs were created using the self-assembling process for 4 weeks, as described above. After the initial 4 weeks of culture, 24 constructs were implanted *in vivo* for an additional 4 weeks, while six constructs were tested immediately after the initial 4 weeks of *in vitro* culture. In parallel, six constructs were left to culture *in vitro* for an additional 4 weeks to compare the effects of *in vitro* incubation vs *in vivo* implantation. A 1.5 cm incision was formed on the dorsal side of the mice under general anesthesia. Two bilateral punches were created on either side of the

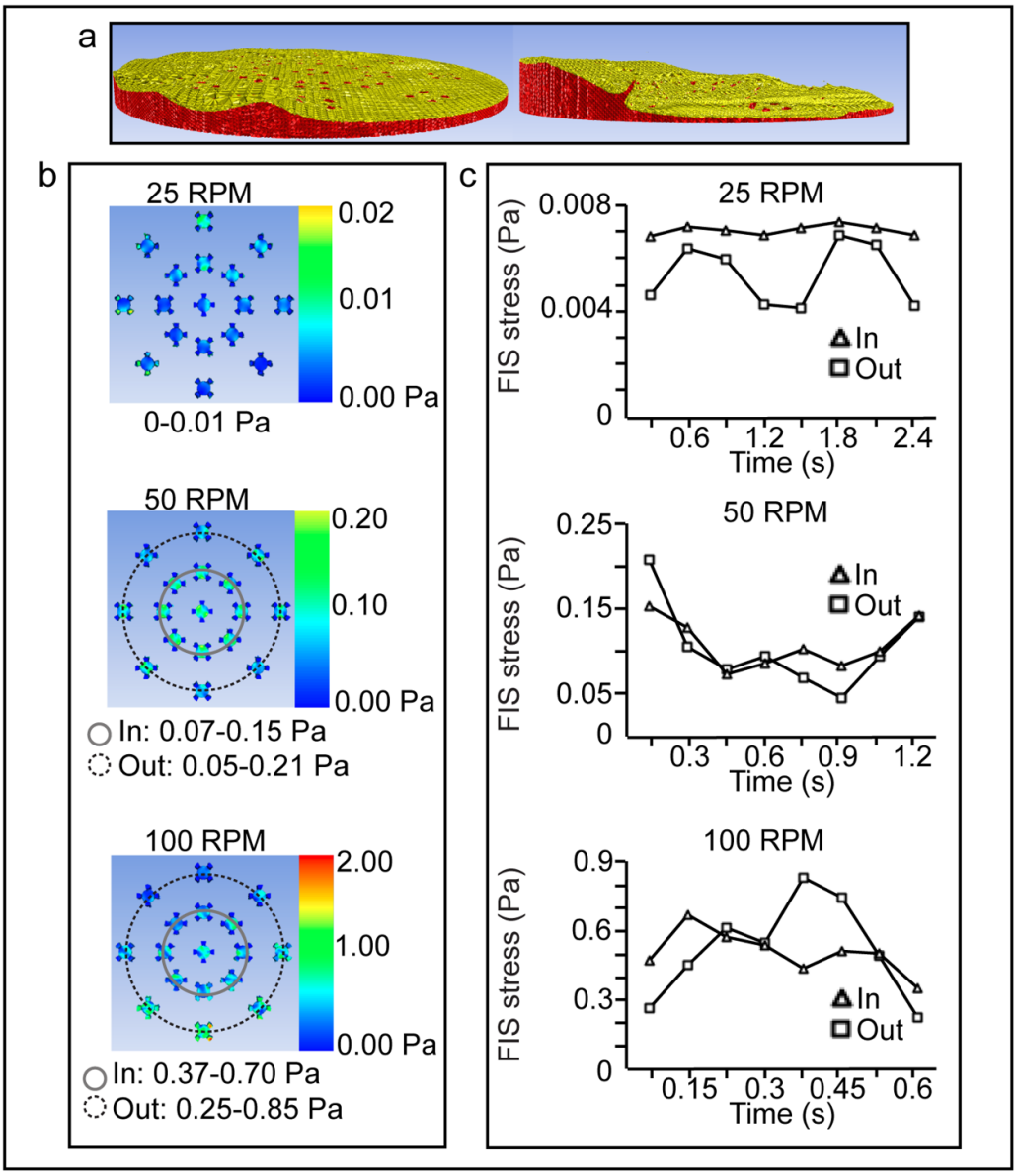

Figure 3. Computational fluid dynamics (CFD) was used to predict the magnitude of shear stress created in the FIS stress device. (a) Snapshots of waveforms of the fluid flow created in the FIS stress device at 25 RPM (left) and 100 RPM (right) on the orbital shaker as predicted by CFD models. (b) CFD modeling of the shear stress distribution in the FIS stress device during stimulation. At 50 and 100 RPM, constructs placed in the inner circle of the FIS stress device experience a slightly different shear stress magnitude range than constructs placed in the outer circle. (c) FIS stress experienced by a construct at varying time points of one orbital shaker cycle.

mice, and a neocartilage construct was placed in each pouch with no mouse receiving two constructs from the same group (−FIS Stress/−TL, +FIS Stress/−TL, +FIS/ + TCL). The investigators were not blinded to which constructs each mouse received. Following 4 weeks of implantation, mice were sacrificed, and the constructs were removed for mechanical and biochemical assessment as specified above.

2.11. Statistical analysis

Analysis of variance and Tukey's *post hoc* tests were used to compare biochemical and mechanical data for multiple group comparisons. Data are presented as mean + standard deviation. Six constructs were used per group to determine the optimal FIS stress stimulation regimen (0.05–0.21 Pa for 12 d). All six constructs were used for biochemical analysis and mechanical testing. Five constructs per group were used in the human neocartilage study to determine mechanical properties, and four constructs were used to determine biochemical properties. For RNA-Seq analysis and RT-PCR verification, four constructs per group were used. Four constructs per group were used in the *in vivo* animal study.

3. Results

3.1. A FIS stress device generated shear stress ranging from 0–0.85 Pa on self-assembled neocartilage

A device capable of inducing FIS stress stimulation on 5 mm diameter, self-assembled neocartilage

constructs was designed (figure 2). CFD modeling was employed to relate fluid flow to ranges of FIS stress magnitudes (figures 3(a)–(c)). The CFD models predicted that the FIS stress device could induce a shear stress range of 0–0.01 Pa at 25 RPM, 0.07–0.15 Pa and 0.05–0.21 Pa at 50 RPM, and 0.37–0.70 Pa and 0.25–0.85 Pa at 100 RPM at different locations (figure 3(b)). Figure 3(c) shows a detailed account of the shear stress experienced by the constructs through time. Each plot represents the time it takes for one full rotation of the orbital shaker. The constructs placed in the inner circle of the FIS stress device experienced slightly different shear stress magnitude ranges than constructs placed in the outer circle. By using an orbital shaker to apply FIS stress, magnitude and frequency of FIS stress loading cannot be studied independently; the frequency of FIS stress loading increases with increasing FIS stress magnitude. It was found that the FIS stress device is capable of imparting shear stress at multiple orders of magnitude on tissue-engineered constructs. Thus, we designed, developed, and implemented a device that successfully applies multiple ranges of FIS stress to neotissues.

3.2. An optimal range of FIS stress, 0.05-0.21 Pa, improved the compressive modulus of neocartilage derived from bovine articular cartilage chondrocytes by 450%

Of the five ranges of FIS stress magnitude that were considered in this study, 0.05–0.21 Pa was found to result in significantly improved construct characteristics. In spite of previous studies indicating that shear stress might lead to degraded neocartilage [1, 19, 20, 31], the aggregate modulus of constructs stimulated by 0.05–0.21 Pa of FIS stress (379 $\pm$ 76 kPa) improved to the level of native tissue [32]. Specifically, constructs that were stimulated with FIS stress for 6 d improved by 450% ($p < 0.05$) (figure 3(a), supplementary table 1) compared to the aggregate modulus of statically cultured controls (98 $\pm$ 25 kPa). This makes FIS stress a promising mechanical loading strategy to produce robust articular cartilage. Interestingly, other ranges of FIS stress decreased construct aggregate modulus values; samples stimulated with 0–0.01 Pa or 0.25–0.85 Pa yielded aggregate modulus values of 44 $\pm$ 21 kPa and 95 $\pm$ 36 kPa, respectively (figure 4(a), supplementary table 1). These findings suggest that although some ranges of shear stress can be harmful to neocartilage, self-assembled neocartilage compressive properties can be improved using a FIS stress magnitude between 0.05–0.21 Pa (figure 4(a), supplementary table 1).

Optimization of the duration of an applied mechanical stimulus is necessary for mechanical stimulation studies. We also investigated the duration of FIS stress stimulation for 12 d at 50 and 100 RPM. A FIS stress stimulation lasting 12 d at 50 RPM was found to yield increased tensile properties, with a tensile Young's modulus of 1.87 $\pm$ 0.59 MPa ($p < 0.05$, over unstimulated controls) and ultimate tensile strength (UTS) of 0.60 $\pm$ 0.15 MPa ($p < 0.05$, over unstimulated controls) (figures 4(b) and (c), supplementary table 1). Thus, we discovered the optimal FIS stress stimulation regimen to be within the range of 0.05–0.21 Pa implemented for 12 d.

In terms of biochemical properties, glycosaminoglycan, collagen, and DNA content were quantified and normalized to dry weight. Glycosaminoglycan content was not shown to increase or decrease in response to FIS stress stimulation for any of the ranges or durations of shear stress that were tested. (Supplementary tables 1(a)–(d)) Collagen content was also not affected by the implementation of FIS stress stimulation. (Supplementary tables 1(a)–(d)) This suggests that the improvements seen in mechanical properties are likely due to crosslinking of fibers. To determine if improvement in mechanical properties was due to an increase in cell quantities, cell growth was measured indirectly using a DNA quantification assay. The DNA/%DW of neocartilage constructs was not affected by FIS stress stimulation. (supplementary tables 1(a)–(d))

3.3. FIS stress led to recapitulation of native tissue fiber density

To verify, visualize, and assess the improvements in extracellular matrix-level fiber organization stemming from FIS stress stimulation, we employed scanning electron microscopy to look at the surface of the neocartilage constructs. Fiber density on the constructs stimulated with the optimal FIS stress regimen was significantly higher than in statically cultured control constructs (figures 5(a) and (b)). Specifically, the fiber density of FIS stress-stimulated constructs improved to 88 $\pm$ 3% from 61 $\pm$ 3% of unstimulated constructs ($p < 0.05$). FIS stress stimulation served to increase extracellular matrix properties and, ultimately, led to the enhancement of mechanical properties.

To ensure that the fiber density observed on the surface of the neocartilage constructs was uniform throughout the inside of the construct, histological staining of top-to-bottom cross-sections was performed. Safranin O staining was more pronounced in neocartilage constructs stimulated with FIS stress, suggesting an increase in proteoglycan content. Furthermore, the stain was uniform throughout FIS stress stimulated constructs, which suggests that the beneficial effects of FIS stress are not localized to the surface of the neocartilage (figure 5(c)).

3.4. A combination of FIS stress and bioactive factors generated additive enhancements in mechanical properties, yielding 1.9- to 3.6-fold improvements over unstimulated controls

Once the optimal FIS stress loading regimen was identified, we investigated the effects of FIS stress

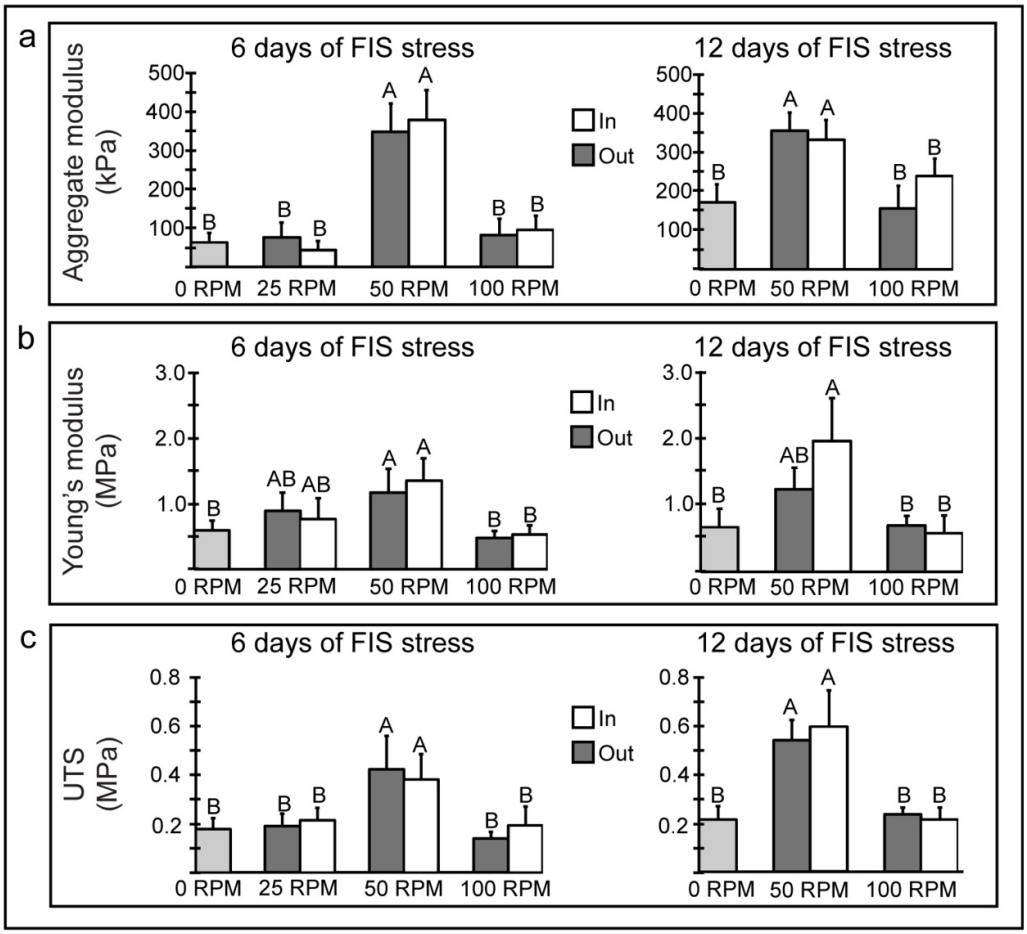

Figure 4. An optimized regimen of FIS stress was found to yield superior mechanical properties of neocartilage. The mechanical properties, (a) aggregate modulus, (b) Young's modulus, and (c) ultimate tensile strength, of unstimulated neocartilage or stimulated with three different ranges of FIS stress. (a)–(c) The position of constructs on the FIS stress device was also investigated (in vs. out), as well as duration of FIS stress stimulation (6 vs. 12 d) One-way analysis of variance ($p < 0.05$) was performed across all groups and letters placed on top of bar graphs indicate statistical significance amongst groups.

stimulation in combination with growth factor TGF-β1, and matrix cross-linking agent, lysyl oxidase like 2 (LOXL2) [33–35]. These bioactive factors, alone or in combination, have previously been shown to enhance tensile and compressive properties in both scaffold-based and scaffold-free neocartilages [33]. Thus, it was of interest to determine if FIS stress stimulation worked in tandem with bioactive factors to further enhance neocartilage properties.

When the bioactive factors were used in combination with FIS stress stimulation (0.05–0.21 Pa for 12 d), both mechanical and biochemical properties of the neocartilage exhibited additive improvements (supplementary table 2(a). In particular, collagen content of neocartilage stimulated with both FIS stress and bioactive factors was improved to 24 ± 2%/DW compared to FIS stress only constructs, 14 ± 2%/DW ($p < 0.001$), and to bioactive factors only constructs, 20 ± 3%/DW ($p < 0.006$). Furthermore, FIS stress in combination with growth factors resulted in a 35% increase in aggregate modulus ($p < 0.002$) and a 56% increase in GAG content over bioactive factors alone ($p < 0.001$). Overall, FIS stress stimulation, combined with bioactive agents, yielded significant improvements in neocartilage properties over non-stimulated controls and significant increases over either form of stimulation alone.

We also assessed the stability of neocartilage properties *in vitro* for 8 weeks. We tissue-engineered constructs using the self-assembling process and after 7 d of initial culture, applied either FIS stress (0.05–0.21 Pa for 12 d), FIS stress + bioactive factors, or no stimulation. In particular, the mechanical properties of constructs stimulated with FIS stress + bioactive factors were improved after 8 weeks *in vitro* with a 197% increase in aggregate modulus ($p < 0.001$), 194% increase in Young's modulus ($p < 0.001$), and a 361% improvement in UTS ($p < 0.002$) over unstimulated controls (supplementary table 2(b)). The consistent trends of elevated compressive and tensile properties in both 4- and 8-week models were encouraging for the application of FIS stress + bioactive factors in *in vivo* studies.

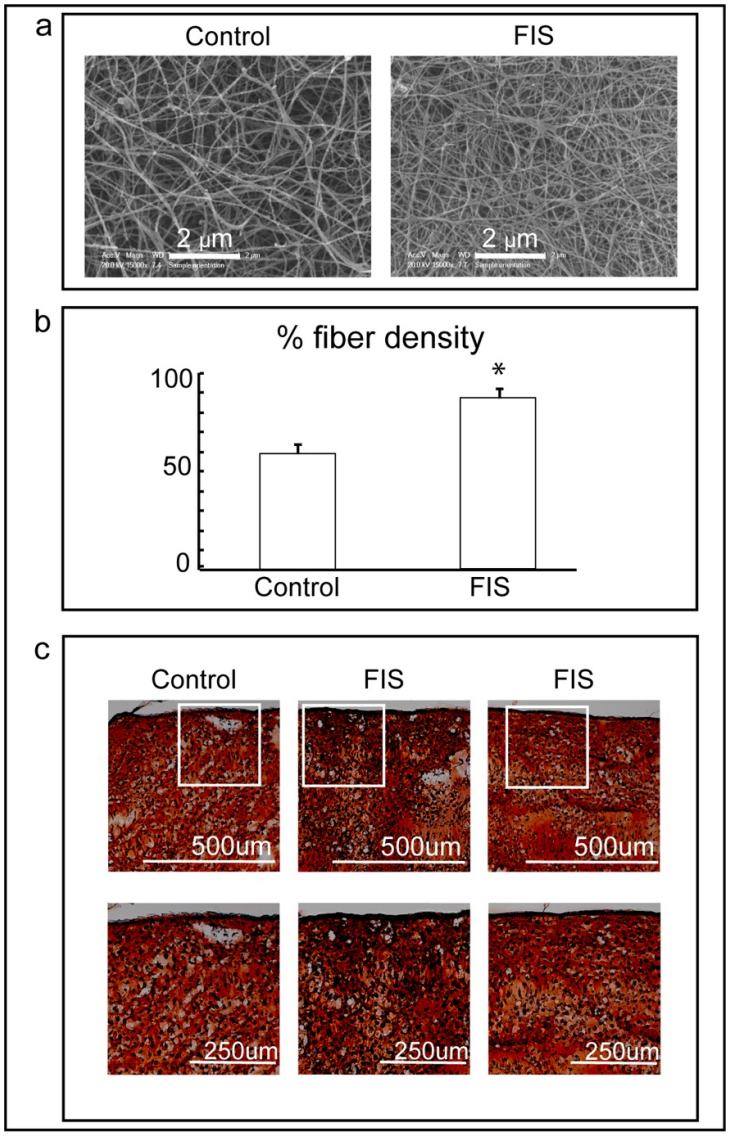

Figure 5. Neocartilage stimulated with FIS stress becomes more fibrous. (a) Scanning electron microscopy images of neocartilage cultured with or without FIS stress showed an increase in the fiber density of the extracellular matrix of stimulated constructs. (b) The fiber density of neocartilage as observed via scanning electron microscopy was quantified by processing scanning electron microscopy images through imagej software. (c) Staining of proteoglycans in neocartilage constructs with a Safranin O stain.

3.5. Implanted neocartilage treated with a combination of FIS stress and bioactive factors remodeled in vivo, yielding a 122% increase in collagen content and 168% increase in Young's modulus

We assessed the stability of neocartilage properties *in vivo* by performing subcutaneous implantation of constructs stimulated (1) without FIS stress, (2) with FIS stress, or (3) with FIS stress + bioactive factors in athymic mice. The neocartilage was implanted for 4 weeks after initial *in vitro* culture duration of 4 weeks. Compared to those maintained *in vitro, in vivo* neocartilage exhibited significant histological, biochemical, and mechanical differences (figures 6(a)–(d), supplementary table 3). Biochemical assays revealed the *in vivo* remodeling of extracellular matrix toward native tissue values across all construct groups, but particularly in neocartilage stimulated with FIS stress + bioactive factors. For example, constructs stimulated with FIS stress + bioactive factors exhibited a 122% increase in collagen content ($p < 0.001$) and a 30% decrease in GAG content ($p < 0.001$) compared to *in vitro* counterparts. Because the self-assembling process initially leads to higher GAG content and lower collagen content than native tissue, increased levels of collagen content and decreased levels of GAG content after implantation suggest that the neocartilage is remodeling and maturing (figure 6(d)) [8, 36].

The mechanical characteristics of stimulated and unstimulated implanted tissues improved, suggesting that neocartilage undergoes *in vivo* maturation. This observation is in accordance with previous studies on implanting neocartilage [7, 34, 37]. In our study, the tensile Young's modulus of unstimulated constructs improved by 168% after implantation ($p < 0.002$) but

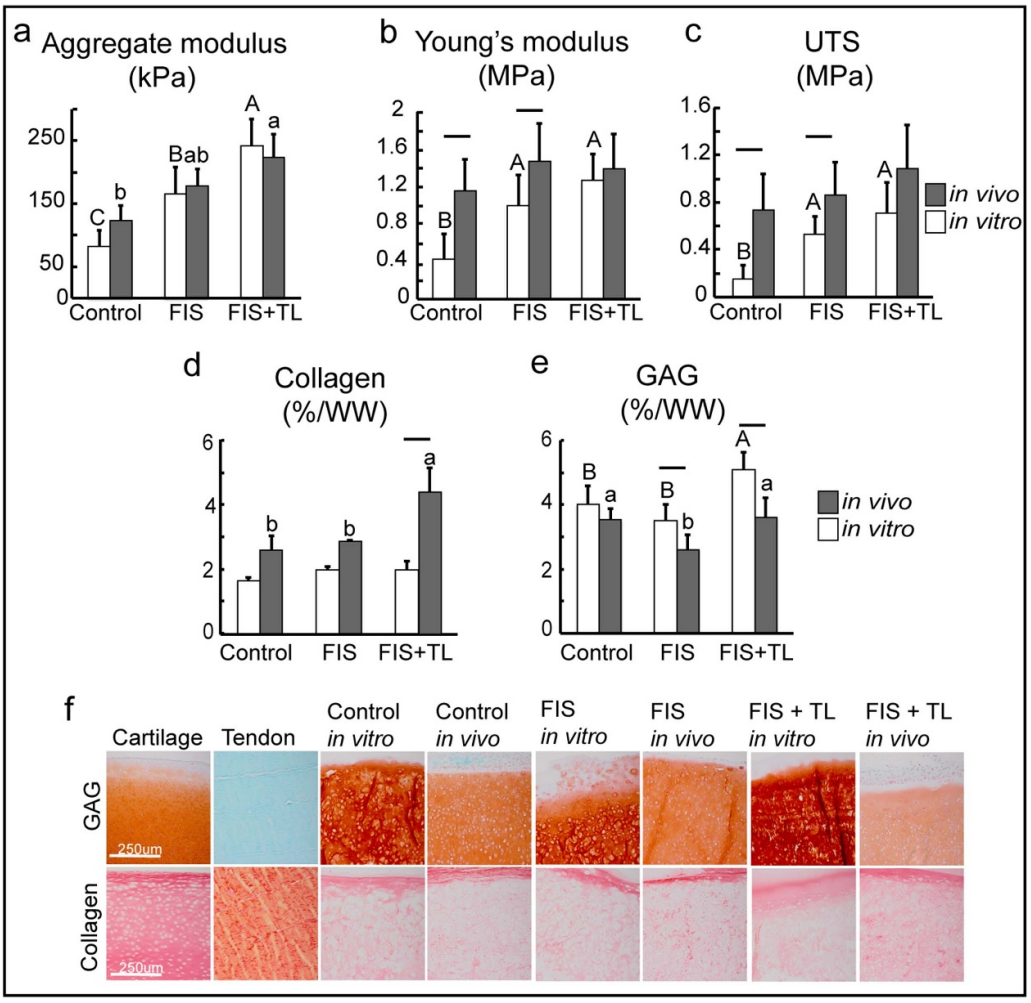

Figure 6. Neocartilage stimulated with FIS stress and implanted *in vivo* remodels and matures. Neocartilage was cultured *in vitro* for an initial 4 weeks and then either implanted for an additional 4 weeks or kept *in vitro* for an additional 4 weeks. Mechanical testing of neocartilage showed that both tensile and compressive characteristics either improved or remained the same after *in vivo* implantation. (a) Aggregate modulus, (b) Young's modulus, (c) ultimate tensile strength (UTS). The biochemical properties of neocartilage showed that it remodels and matures *in vivo*. (d) Collagen content, (e) glycosaminoglycan (GAG) content. (a)–(e) Lower-case letters placed on top of bar graphs indicate statistical significance amongst *in vivo* groups (one-way analysis of variance). Capital letters placed on top of bar graphs indicate statistical significance amongst *in vitro* groups (one-way analysis of variance). Line on top of bars denotes differences between *in vivo* and *in vitro* constructs (student's t-test; $p < 0.05$). (f) Histological staining for collagen and GAG organization showed that after implantation, a more uniform distribution of collagen content was present, GAG density appeared more similar to native tissue, and chondrocytes were organized in a columnar fashion. All of these characteristics are reminiscent of native tissue.

did not surpass the Young's modulus of implanted, treated groups. The UTS of control neocartilage and neocartilage stimulated with FIS stress improved after implantation, while the neocartilage stimulated with both FIS and bioactive factors did not significantly change after implantation. The histology showed that the *in vivo* environment induced cellular organization and morphology changes in all construct groups; after implantation, chondrocytes oriented themselves in a columnar fashion and exhibited pronounced lacunae (figure 6(f)). Collectively, these data show that the subcutaneous implantation of neocartilage constructs not only maintains and enhances the properties of neocartilage stimulated with FIS stress and FIS stress + bioactive factors toward those of native articular cartilage, but also results in neocartilage constructs that are morphologically reminiscent of native articular cartilage.

3.6. Human neocartilage, stimulated with FIS stress, increased mechanical properties by 72%–201% over unstimulated controls

The ultimate goal of tissue engineering is to create tissues for use in human implantation, but improvements seen with bovine cells do not necessarily translate to passaged human chondrocytes. Furthermore, there are few studies, if any, where shear stress has been used to engineer human articular cartilage. When creating human neocartilage, bioactive factors, TGF-β1, LOXL2, and C-ABC, were used successfully during tissue culture [15]. It was,

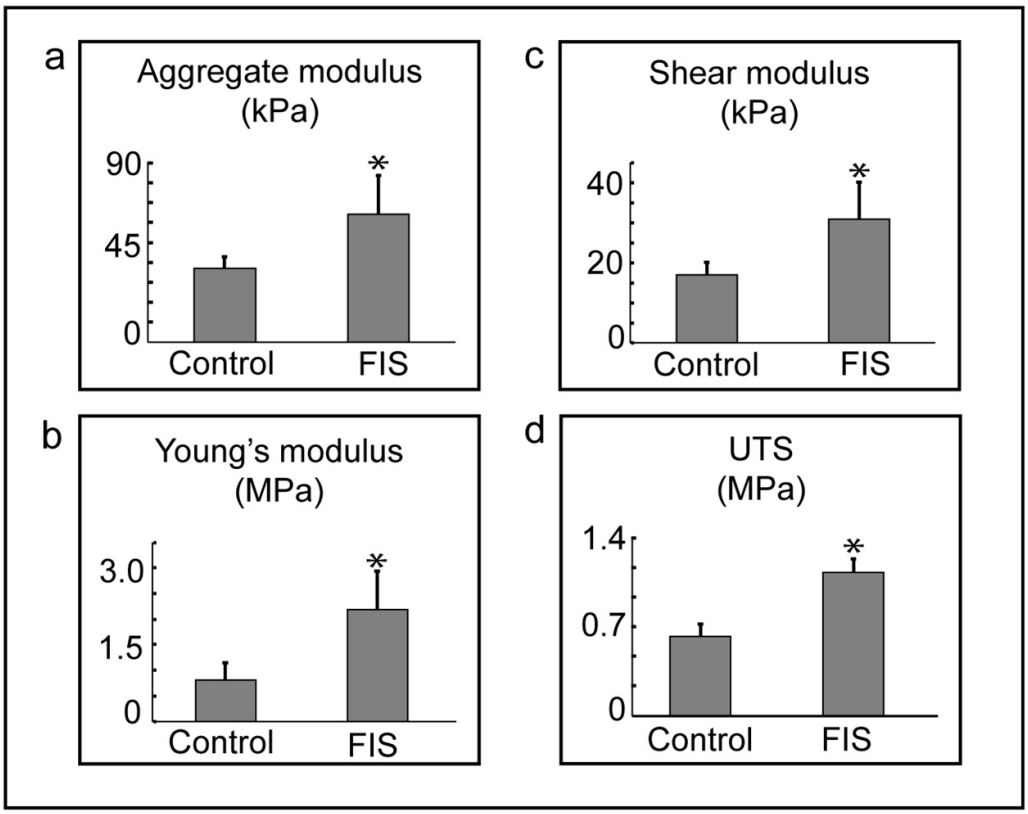

Figure 7. The mechanical properties of human neocartilage constructs stimulated with the optimized FIS stress regimen were improved over controls. The following properties of neocartilage constructs were tested and compared (student's t-test, $p < 0.05$): (a) Aggregate modulus, (b) shear modulus, (c) Young's modulus, and (d) ultimate tensile strength (UTS).

thus, of interest to determine if FIS stress stimulation would synergize with these bioactive factors to produce human neocartilage. Articular chondrocytes were harvested, expanded up to passage three, redifferentiated with aggregate culture, and both groups were placed into self-assembly with the addition of bioactive factors [15]. Neocartilage constructs were then separated into two groups, with or without FIS stress stimulation.

As in our bovine studies, the human neocartilage treated with FIS stress improved in mechanical functionality. In terms of compressive properties, the addition of FIS stress during tissue engineering yielded an aggregate modulus 72% larger ($p < 0.008$) and a shear modulus 66% larger ($p < 0.05$) than controls (figures 7(a) and (b), supplementary table 4). FIS stress improved the tensile Young's modulus by 201% ($p < 0.02$) and the UTS by 122% ($p < 0.008$) over controls (figures 7(c) and (d), supplementary table 4). Although bovine neocartilage display much higher compressive properties than those of human neocartilage, these data are consistent with previous mechanical stimulation strategies applied to human neocartilage [13], and illustrate the potential of using FIS stress in engineering human neocartilage. Optimization of a FIS stress regimen is an effective method to drive human neocartilage toward native characteristics.

3.7. FIS stress stimulation upregulated genes encoding a mechanosensitive complex of primary cilia

Toward elucidating the mechanism behind the improved properties of neocartilage stimulated with FIS stress, we performed RNA-Seq to capture genes that may be responsible. We hypothesized that FIS stress-induced improvements might not only be a result of increased nutrient perfusion and transport of waste, but also the result of complex cellular signaling events and matrix remodeling initiated by mechanotransduction. RNA-Seq and subsequent differential expression analysis revealed the upregulation of 694 genes and the downregulation of 613 genes in FIS stress-stimulated neocartilage compared to unstimulated controls (figure 8(a)). Using the NIH's DAVID and Cytoscape to analyze the data obtained from RNA-Seq, we determined the major gene categories that appeared modified in response to FIS stress stimulation. These include mechano-regulated ion channels and complexes found on the primary cilia of cells, growth factors, extracellular matrix organization proteins, and extracellular matrix assembly proteins (supplementary figure 1).

From the genes that were shown to be altered by FIS stress using RNA-Seq, of particular interest was the upregulation of polycystin 1 (PC1) and 2 (PC2), which are encoded by PKD1 and PKD2

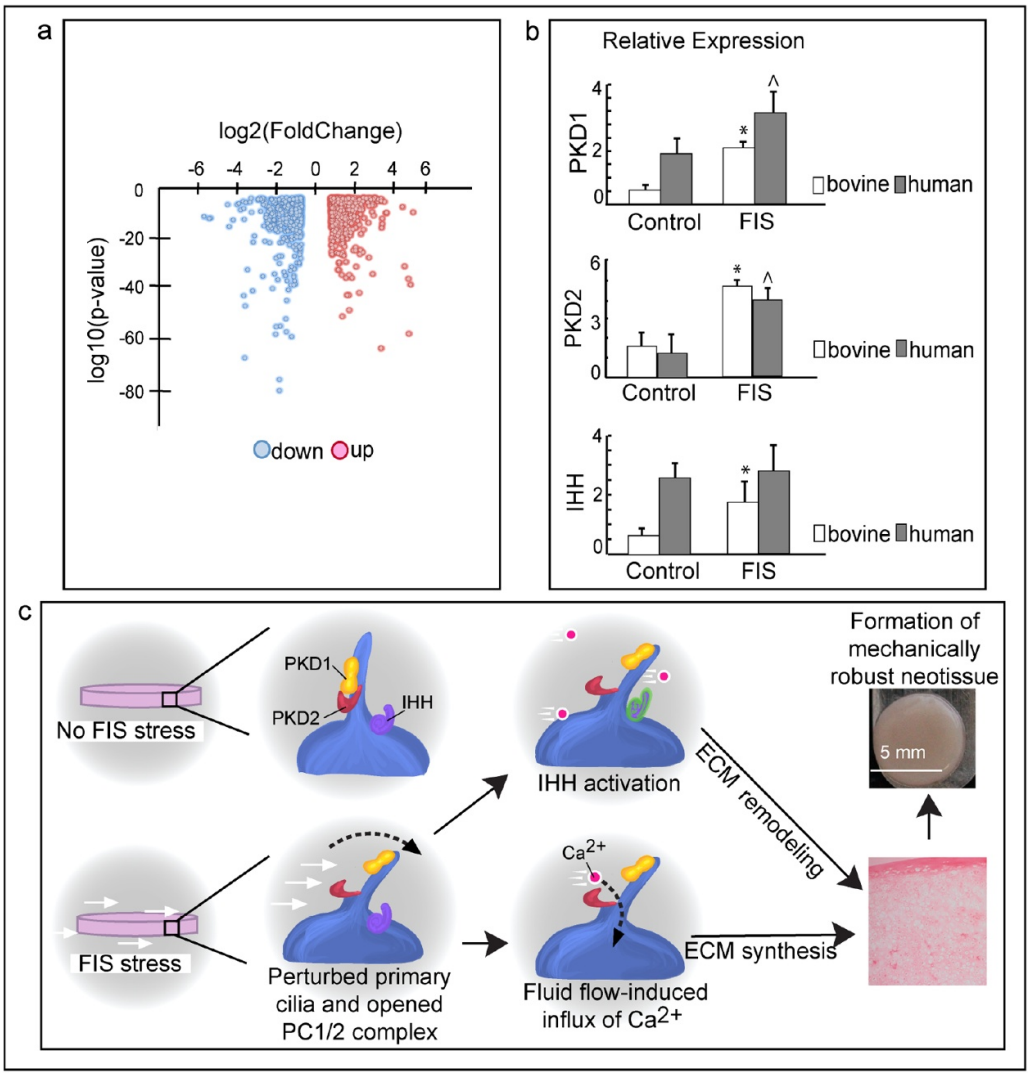

Figure 8. The modes of action of FIS stress. (a) A volcano plot generated from RNA-Seq and differential expression analysis is shown. Genes that were found to be upregulated in FIS stress-stimulated constructs are in red, and downregulated genes are in blue. Only genes that were found to have higher than a 2-fold change difference and a p-value < 0.05 are shown. (b) The relative expressions of genes of interest IHH, PKD1, and PKD2 to the housekeeping gene are shown for control and FIS stress-stimulated constructs (Student's t-test, $p < 0.05$, * shows significance for bovine, ^ shows significance for human). (c) A schematic showing how FIS stress leads to robust neocartilage. When FIS stress is applied to the construct, the primary cilia of chondrocytes are perturbed and the PC1/2 complex is opened, allowing the influx of Ca^{2+} ions and an increase in IHH signaling. This leads to a cascade of signaling events that initiate extracellular matrix synthesis and remodeling which result in mechanically robust neocartilage constructs.

respectively, to form an ion-gated complex. RNA-Seq data were confirmed by RT-PCR for both bovine-derived and human-derived neocartilage constructs. We found that PKD1 and PKD2 were significantly upregulated in both bovine and human neocartilage stimulated with FIS stress (figure 8(b)). This suggests that FIS stress induces the formation of more PC1/2 complexes on primary cilia, leading to increased sensitivity to fluid flow. Primary cilia are known to be necessary modulators of Indian Hedgehog (IHH) signaling in chondrocytes and other cell types [38, 39]. In chondrocytes, IHH is salient in regulating developmental features such as proliferation and maturation [40]. Therefore, we also investigated and verified the upregulation of IHH expression in the bovine-derived neocartilage constructs via RT-PCR (figure 8(b)). The activation of the PC1/2 complexes by fluid flow perturbation would result in a greater influx of Ca^{2+} ions, than unstimulated chondrocytes [41, 42], initiating a cascade of upregulated extracellular matrix producing and remodeling genes and proteins in chondrocytes [43–45], leading to the formation of mechanically robust neocartilage (figure 8(c)).

4. Discussion

In this series of six studies, we investigated the use of FIS stress to enhance the formation of tissue-engineered cartilage using the self-assembling process. In the first study, we designed a FIS stress device and performed CFD to predict the ranges

of FIS stress produced in the device. We determined that the FIS stress device could impart separate ranges of shear stress on the neocartilage constructs, spanning multiple orders of magnitude: 0–0.01 Pa, 0.07–0.15 Pa, 0.05–0.21 Pa, 0.37–0.70 Pa, and 0.25–0.85 Pa. For our second study, we found that neocartilage benefits from an optimal FIS stress of 0.05–0.21 Pa, improving mechanical and biochemical properties over control groups as well as other shear stress experimental groups. In the third study, we carried on the use of the optimal FIS stress loading conditions and combined with bioactive agents to yield additive improvements on the biochemical and mechanical properties of neocartilage. In the fourth study, we implanted the neocartilage constructs in athymic mice and found that they remodeled and matured *in vivo* toward native characteristics. In the fifth study, we successfully translated the optimal FIS stress stimulation loading conditions to human cartilage tissue culture. Finally, in the sixth study, we elucidated a complex on the primary cilia of both human and bovine chondrocytes that is sensitive to fluid flow and may be responsible for the observed improvements. This work is significant because it presents a comprehensive examination of how FIS stress improves neocartilage formation based on mechanotransduction through the primary cilia. Importantly, we showed that the magnitude of the applied FIS stress can be tuned to elicit large improvements in mechanical, structural, and biochemical properties of tissue-engineered constructs.

There is a lack of clarity on the effects of FIS stress on tissues. On one hand, fluid flow is known to increase nutrient perfusion and waste transport which is conducive to cellular health [46]. However, with fluid flow comes FIS stress, which at high magnitudes may lead to pathologic tissue states in some cell types. For example in human chondrocytes, high-shear environments have been shown to cause apoptosis and increases in proinflammatory factors [5, 47]. Juxtaposed against these results, cartilage tissue culture that includes a shear stress regimen has been shown to lower coefficient of friction [17, 18]. Our work here shows that, during cartilage tissue culture, shear stress can be harmful at high shear stress levels (>0.21 Pa), and beneficial for mechanical and biochemical properties within the range of 0.05–0.21 Pa. This is in accordance with other tissue types such as vascular tissue, where shear stress less than 0.5 Pa is conducive to angiogenesis [46], but at 20 Pa, it leads to atherosclerosis [48]. This supports the hypothesis that the shear stress magnitude implemented during tissue culture can be optimized to provide improvements in neotissue properties.

When culturing neotissues and cells under physiologically relevant mechanical cues, it should be noted that native cells experience different magnitudes of mechanical stress compared to the surrounding tissue matrix. For native articular cartilage of the knee, biphasic models incorporating finite element analysis of interstitial fluid flux around chondrocytes show that the extracellular matrix experiences peak shear stresses of 55 kPa due to tissue deformation under physiological conditions. However, the chondrocytes dwelling in the tissue, which are protected by the pericellular and extracellular matrices, experience FIS stress at around 0.065 Pa [49]. The shear stress experienced by native articular chondrocytes of the knee is comparable to the range of FIS stress found here to produce the most improved neocartilage constructs (0.05–0.21 Pa), thus providing indirect validation of the computational model [49]. The self-assembled neocartilage constructs used in the studies presented are dense with chondrocytes in comparison to native articular cartilage and are not as well shielded by a collagenous matrix from FIS stress. Therefore, we believe that the chondrocytes residing in the self-assembled neocartilage are experiencing similar shear stress magnitudes as they would in a native environment.

Histological staining showed that the fiber density of the neocartilage stimulated with FIS stress is uniform throughout. Because only the chondrocytes on the surface of the neocartilage constructs are exposed to the FIS stress imparted by the device, it is possible that the chondrocytes within the neocartilage are experiencing paracrine effects. Further experiments need to be performed under well-controlled shear regiments to fully understand the effects of paracrine signaling and to differentiate them from mechanotransduction. Additionally, it is possible that the improvements in neocartilage constructs stimulated with FIS stress may be partly attributed to increased nutrient diffusion and oxygen distribution. Previous studies have explored the use of spinner flasks and have found that neocartilage that remained in fluid flow for 6 weeks was inferior in terms of glycosaminoglycan content and collagen content when compared to neocartilage that experienced fluid flow for 2 weeks of culture [50]. A separate study showed that a continuous fluid flow applied on neocartilage for 3 d increased collagen type II deposition [18]. Interestingly, the shear stress applied in the previous study, 0.1 Pa, is on the same order of magnitude as the optimal FIS stress found here, 0.05–0.21 Pa. These studies further support the hypothesis that an optimal shear stress magnitude is important for the successful application of FIS stress on neotissues.

For other forms of mechanical stimulation on chondrocytes, mechanotransduction pathways, such as TRPV4 activation in tension, have been implicated [13]. To this list we now add the activation of the mechanically gated complex PC1/2 via FIS stress. In osteoblasts and osteocytes, this mechanically gated complex allows for fluid flow-induced influx of Ca^{2+} ions [51]. For chondrocytes, it has been shown that the PC1/2 complex is involved in mechanotransducing compressive forces [14]. Because chondrocyte

cilia have been previously observed [14, 51], and because genomic data suggest that the PC1/2 complex exists on chondrocyte primary cilia [39, 42, 51], our findings add to this body of work in implicating the PC1/2 complex in mechanotransducing FIS stress in chondrocytes as well. Although further study, such as antagonizing primary cilia to show loss or gain of function, is necessary to fully confirm FIS stress modes of action on chondrocytes, this series of studies showed that shear stress stimulation acts via mechanotransduction to increase extracellular matrix content and to enhance mechanical properties.

In vivo, FIS stress-stimulated constructs were shown to outperform statically cultured constructs. There is a dearth of studies examining *in vivo* functionality of constructs stimulated with either direct shear stress or FIS stress [12]. *In vitro* studies show that direct shear stress enhances *in vitro* integration [52], as well as reduced friction coefficients [53]. Our work using FIS stress showed its superior ability in cartilage to effect remodeling and maturation that carry over to the *in vivo* environment. These effects were manifested in increases in collagen content, chondrocyte organization, and pronounced lacunae of FIS stress-stimulated constructs. Although orthotopic *in vivo* implantation studies are necessary as a next step to validate functional superiority, this series of studies yielded promising results for the translational potential of neocartilage stimulated with FIS stress.

Here, we reported the design and use of a shear-loading device that successfully applies fluid flow-induced shear stress to tissue-engineer cartilage with enhanced compressive, shear, tensile, structural, and biochemical properties. The device, capable of inducing FIS stresses spanning 0–0.85 Pa, is potentially suitable for both scaffold-based and scaffold-free culture of neotissues, including tissue engineered bone, muscle, tendon, ligament, and fibrocartilage. For articular cartilage tissue engineering, we identified a FIS stress range, 0.05–0.21 Pa, that improves mechanical properties by 1.9- to 3.6-fold via a primary cilia-based mechanosensitive complex. To implement this strategy for other tissue types in the future, one must identify optimal loading parameters for specific tissue culture conditions, including the use of scaffolds. In self-assembled neocartilage, this series of studies showed that the optimized regimen of FIS stress alone yields large enhancements in neocartilage properties. When a cocktail of bioactive agents was combined with FIS stress, further additive improvements in both mechanical and biochemical characteristics of neocartilage were noted. Toward translating these findings to human neocartilage, human articular chondrocytes exposed to FIS stress responded in a robust manner resulting in the formation of appropriately stiff and strong tissue-engineered cartilage, increasing mechanical properties by 0.7- to 2-fold. Together, these data demonstrated the beneficial contribution of FIS stress to neocartilage tissue culture.

Acknowledgments

We express our gratitude to the Genomic High Throughput Facility at UCI for assistance and expertise with genome sequencing. In particular, we appreciate the assistance provided by Carlos Guzman with differential expression analysis and large data sets.

Funding

NIH R01AR067821

Author contributions

EYS designed study, completed experiments and data analysis, and wrote manuscript. AA designed study, completed experiments and data analysis, and wrote manuscript. NP designed study and completed experiments and data analysis. EB completed experiments and data analysis. HK completed experiments and data analysis. JCH designed study and edited manuscript. KAA designed study and edited manuscript.

Conflict interests

No competing interests exist.

ORCID iD

E Y Salinas
https://orcid.org/0000-0002-0343-9444

References

[1] Goodwin T J, Prewett T L, Wolf D A and Spaulding G F 1993 Reduced shear stress: a major component in the ability of mammalian tissues to form three-dimensional assemblies in simulated microgravity *J. Cell. Biochem.* **51** 301–11
[2] 2016 Osteoarthritis research society international: OA as a serious disease *White Paper* submited to U.S Food and Drug Administration https://www.oarsi.org/sites/default/files/docs/2016/oarsi_white_paper_oa_serious_disease_121416_1.pdf
[3] Archambault J M, Elfervig-Wall M K, Tsuzaki M, Herzog W and Banes A J 2002 Rabbit tendon cells produce MMP-3 in response to fluid flow without significant calcium transients *J. Biomech.* **35** 303–9
[4] Smith R L, Trindade M C D, Ikenoue T, Mohtai M, Das P, Carter D R, Goodman S B and Schurman D J 2000 Effects of shear stress on articular chondrocyte metabolism *Biorheology* **37** 95–107
[5] Healy Z R, Zhu F, Stull J D and Konstantopoulos K 2008 Elucidation of the signaling network of COX-2 induction in sheared chondrocytes: COX-2 is induced via a Rac/MEKK1/MKK7/JNK2/c-Jun-C/EBPβ-dependent pathway *Am. J. Physiol. Cell Physiol.* **294** C1146–57
[6] Kwon H, Paschos N K, Hu J C and Athanasiou K A 2016 Articular cartilage tissue engineering: the role of signaling molecules *Cell. Mol. Life Sci.* **73** 1173–94
[7] Athanasiou K A, Eswaramoorthy R, Hadidi P and Hu J C 2013 Self-organization and the self-assembling process in tissue engineering *Annu. Rev. Biomed. Eng.* **15** 115–36

[8] Hu J C and Athanasiou K A 2006 A self-assembling process in articular cartilage tissue engineering *Tissue Eng.* **12** 969–79

[9] Athanasiou K A, Darling E M, Hu J C, DuRaine G D and Reddi A H 2017 *Articular Cartilage* 2 edn (Boca Raton, FL: CRC Press)

[10] Huey D J, Hu J C and Athanasiou K A 2012 Unlike bone, cartilage regeneration remains elusive *Science* **338** 917–21

[11] Langer R and Vacanti J P 1993 Tissue engineering *Science* **260** 920

[12] Salinas E Y, Hu J C and Athanasiou K A 2018 A guide for using mechanical stimulation to enhance tissue-engineered articular cartilage properties *Tissue Eng. Part B: Rev.* **24** 345–58

[13] Lee J K, Huwe L W, Paschos N, Aryaei A, Gegg C A, Hu J C and Athanasiou K A 2017 Tension stimulation drives tissue formation in scaffold-free systems *Nat. Mater.* **16** 864

[14] Wann A K, Zuo N, Haycraft C J, Jensen C G, Poole C A, McGlashan S R and Knight M M 2012 Primary cilia mediate mechanotransduction through control of ATP-induced Ca2+ signaling in compressed chondrocytes *Faseb J.* **26** 1663–71

[15] Kwon H, O'Leary S A, Hu J C and Athanasiou K A 2019 Translating the application of transforming growth factor-β1, chondroitinase-ABC, and lysyl oxidase-like 2 for mechanically robust tissue-engineered human neocartilage *J. Tissue Eng. Regen. Med.* **13** 283–94

[16] Bernhard J C and Vunjak-Novakovic G 2016 Should we use cells, biomaterials, or tissue engineering for cartilage regeneration? *Stem Cell Res. Ther.* **7** 56

[17] Gemmiti C V and Guldberg R E 2009 Shear stress magnitude and duration modulates matrix composition and tensile mechanical properties in engineered cartilaginous tissue *Biotechnol. Bioeng.* **104** 809–20

[18] Gemmiti C V and Guldberg R E 2006 Fluid flow increases type II collagen deposition and tensile mechanical properties in bioreactor-grown tissue-engineered cartilage *Tissue Eng.* **12** 469–79

[19] Cherry R S and Papoutsakis E T 1986 Hydrodynamic effects on cells in agitated tissue culture reactors *Bioprocess Eng.* **1** 29–41

[20] Begley C M and Kleis S J 2000 The fluid dynamic and shear environment in the NASA/JSC rotating-wall perfused-vessel bioreactor *Biotechnol. Bioeng.* **70** 32–40

[21] Thomas J M D, Chakraborty A, Berson R E, Shakeri M and Sharp M K 2017 Validation of a CFD model of an orbiting culture dish with PIV and analytical solutions *AIChE J.* **63** 4233–42

[22] Berson R E, Purcell M R and Sharp M K 2008 Computationally determined shear on cells grown in orbiting culture dishes *Oxygen Transport to Tissue XXIX* (Berlin: Springer) pp 189–98

[23] Thomas J M D, Chakraborty A, Sharp M K and Berson R E 2011 Spatial and temporal resolution of shear in an orbiting petri dish *Biotechnol. Prog.* **27** 460–5

[24] Chakraborty A, Chakraborty S, Jala V R, Thomas J M, Sharp M K, Berson R E and Haribabu B 2016 Impact of bi-axial shear on atherogenic gene expression by endothelial cells *Ann. Biomed. Eng.* **44** 3032–45

[25] Mow V C, Kuei S, Lai W M and Armstrong C G 1980 Biphasic creep and stress relaxation of articular cartilage in compression: theory and experiments *J. Biomech. Eng.* **102** 73–84

[26] Setton L A, Zhu W and Mow V C 1993 The biphasic poroviscoelastic behavior of articular cartilage: role of the surface zone in governing the compressive behavior *J. Biomech.* **26** 581–92

[27] Mow V C, Gibbs M C, Lai W M, Zhu W B and Athanasiou K A 1989 Biphasic indentation of articular cartilage—II. a numerical algorithm and an experimental study *J. Biomech.* **22** 853–61

[28] Lu X and Mow V 2008 Biomechanics of articular cartilage and determination of material properties *Med. Sci. Sports Exercise* **40** 193

[29] Cissell D D, Link J M, Hu J C and Athanasiou K A 2017 A modified hydroxyproline assay based on hydrochloric acid in Ehrlich's solution accurately measures tissue collagen content *Tissue Eng. Part C: Methods* **23** 243–50

[30] Heinz S, Benner C, Spann N, Bertolino E, Lin Y C, Laslo P, Cheng J X, Murre C, Singh H and Glass C K 2010 Simple combinations of lineage-determining transcription factors prime cis-regulatory elements required for macrophage and B cell identities *Mol. Cell* **38** 576–89

[31] Trevino R L, Pacione C A, Malfait A-M, Chubinskaya S and Wimmer M A 2016 Development of a cartilage shear-damage model to investigate the impact of surface injury on chondrocytes and extracellular matrix wear *Cartilage* **8** 444–55

[32] Bernhard J C, Hulphers E, Rieder B, Ferguson J, Rünzler D, Nau T, Redl H and Vunjak-Novakovic G 2018 Perfusion enhances hypertrophic chondrocyte matrix deposition, but not the bone formation *Tissue Eng. Part* A **24** 1022–33

[33] Makris E A, MacBarb R F, Paschos N K, Hu J C and Athanasiou K A 2014 Combined use of chondroitinase-ABC, TGF-β1, and collagen crosslinking agent lysyl oxidase to engineer functional neotissues for fibrocartilage repair *Biomaterials* **35** 6787–96

[34] Huey D J and Athanasiou K A 2011 Maturational growth of self-assembled, functional menisci as a result of TGF-β1 and enzymatic chondroitinase-ABC stimulation *Biomaterials* **32** 2052–8

[35] Eyre D R, Weis M A and Wu -J-J 2008 Advances in collagen cross-link analysis *Methods* **45** 65–74

[36] Lee J K, Hu J C, Yamada S and Athanasiou K A 2016 Initiation of chondrocyte self-assembly requires an intact cytoskeletal network *Tissue Eng. Part* A **22** 318–25

[37] Jurvelin J, Buschmann M and Hunziker E 2003 Mechanical anisotropy of the human knee articular cartilage in compression *Proc. Inst. Mech. Eng.* H **217** 215–9

[38] Eggenschwiler J T and Anderson K V 2007 Cilia and developmental signaling *Annu. Rev. Cell Dev. Biol.* **23** 345–73

[39] Rais Y, Reich A, Simsa-Maziel S, Moshe M, Idelevich A, Kfir T, Miosge N and Monsonego-Ornan E 2015 The growth plate's response to load is partially mediated by mechano-sensing via the chondrocytic primary cilium *Cell. Mol. Life Sci.* **72** 597–615

[40] Hilton M J, Tu X, Cook J, Hu H and Long F 2005 Ihh controls cartilage development by antagonizing Gli3, but requires additional effectors to regulate osteoblast and vascular development *Development* **132** 4339

[41] Gargalionis A N, Basdra E K and Papavassiliou A G 2018 Polycystins in disease mechanobiology *J. Cell. Biochem.* **120** 6894–8

[42] Mangolini A, de Stephanis L and Aguiari G 2016 Role of calcium in polycystic kidney disease: from signaling to pathology *World J. Nephrol.* **5** 76–83

[43] Han S-K, Wouters W, Clark A and Herzog W 2012 Mechanically induced calcium signaling in chondrocytes in situ *J. Orthop. Res.* **30** 475–81

[44] Weber J F and Waldman S D 2014 Calcium signaling as a novel method to optimize the biosynthetic response of chondrocytes to dynamic mechanical loading *Biomech. Model Mechanobiol.* **13** 1387–97

[45] Grodzinsky A J, Levenston M E, Jin M and Frank E H 2000 Cartilage tissue remodeling in response to mechanical forces *Annu. Rev. Biomed. Eng.* **2** 691–713

[46] Cunningham K S and Gotlieb A I 2005 The role of shear stress in the pathogenesis of atherosclerosis *Lab. Invest.* **85** 9–23

[47] Wang P, Guan -P-P, Guo C, Zhu F, Konstantopoulos K and Wang Z-Y 2013 Fluid shear stress-induced osteoarthritis: roles of cyclooxygenase-2 and its metabolic products in

inducing the expression of proinflammatory cytokines and matrix metalloproteinases *FASEB J.* **27** 4664–77

[48] Chiu -J-J, Lee P-L, Chen C-N, Lee Chih I, Chang S-F, Chen L-J, Lien S-C, Ko Y-C, Usami S and Chien S 2004 Shear stress increases ICAM-1 and decreases VCAM-1 and E-selectin expressions induced by tumor necrosis factor-α in endothelial cells *Arteriosclerosis Thrombsis Vasc. Biol.* **24** 73–79

[49] Ateshian G A, Costa K D and Hung C T 2007 A theoretical analysis of water transport through chondrocytes *Biomech. Model Mechanobiol.* **6** 91–101

[50] Carver S E and Heath C A 1999 Influence of intermittent pressure, fluid flow, and mixing on the regenerative properties of articular chondrocytes *Biotechnol. Bioeng.* **65** 274–81

[51] Xiao Z S and Quarles L D 2010 Role of the polycytin-primary cilia complex in bone development and mechanosensing *Ann. New York Acad. Sci.* **1192** 410–21

[52] Theodoropoulos J S, DeCroos A J, Petrera M, Park S and Kandel R A 2016 Mechanical stimulation enhances integration in an in vitro model of cartilage repair *Knee Surg. Sports Traumatology Arthroscopy* **24** 2055–64

[53] Grad S, Loparic M, Peter R, Stolz M, Aebi U and Alini M 2012 Sliding motion modulates stiffness and friction coefficient at the surface of tissue engineered cartilage *Osteoarthritis Cartilage* **20** 288–95